Interleukin-10 attenuates renal injury after myocardial infarction in diabetes

Xiaoming Fan, Xiaolu Zhang, Lijun C Liu, Annes Y Kim, Sean P Curley, Xiaohuan Chen, Lance D Dworkin, Christopher J Cooper, Rajesh Gupta

Department of Medicine, University of Toledo - Health Science Campus, Toledo, Ohio, USA

Correspondence to
Dr Rajesh Gupta, Department of Medicine, University of Toledo - Health Science Campus, Toledo, Ohio, USA;
rajesh.gupta@utoledo.edu

XF and XZ contributed equally.

Accepted 12 January 2022

To cite: Fan X, Zhang X, Liu LC, *et al*. *J Investig Med* Epub ahead of print: [*please include* Day Month Year]. doi:10.1136/jim-2021-002008

ABSTRACT

Acute kidney injury (AKI) is a common complication after myocardial infarction (MI) and associated with significant morbidity and mortality. AKI after MI occurs more frequently in patients with diabetes, however, the underlying mechanisms are poorly understood, and specific treatments are lacking. Using the murine MI model, we show that diabetic mice had higher expression of the kidney injury marker, neutrophil gelatinase-associated lipocalin (NGAL), 3 days after MI compared with control mice. This higher expression of NGAL was still significant after controlling for differences in myocardial infarct size between diabetic and control mice. Prior data demonstrate increased cell-free hemoglobin after MI in diabetic mice. Therefore, we investigated heme clearance components, including heme oxygenase 1 (HO-1) and CD163, in the kidneys and found that both HO-1 and CD163 were dysregulated in diabetic mice pre-MI and post-MI. Significantly higher levels of urine iron were also observed in diabetic mice compared with control mice after MI. Next, the renal protective effect of interleukin 10 (IL-10) after MI was tested in diabetic MI. IL-10 treatment demonstrated multiple protective effects after diabetic MI including reduction in acute renal inflammation, upregulation of renal heme clearance pathways, attenuation of chronic renal fibrosis, and reduction in albuminuria after diabetic MI. In vitro, IL-10 potentiated hemoglobin-induced HO-1 expression in mouse bone marrow-derived macrophages and renal proximal tubule (HK-2) cells. Furthermore, IL-10 reduced hemoglobin-induced reactive oxygen species in HK-2 cells and collagen synthesis in mouse embryonic fibroblast cells. We conclude that impaired renal heme clearance pathways in diabetes contribute to AKI after MI, and IL-10 attenuates renal injury after diabetic MI.

Significance of this study

What is already known about this subject?

- Diabetes mellitus is an important risk factor for acute kidney injury (AKI) after myocardial infarction (MI).
- Higher levels of circulating cell-free hemoglobin were observed in diabetic mice compared with non-diabetic control mice after MI.

What are the new findings?

- Diabetic mice had higher expression of renal neutrophil gelatinase-associated lipocalin after MI.
- Dysregulated renal heme protein clearance is observed in diabetic mice pre-MI and post-MI.
- Interleukin 10 (IL-10) potentiates heme protein clearance pathways and protects against renal fibrosis and albuminuria after diabetic MI.
- IL-10 reduces hemoglobin-induced reactive oxygen species in renal proximal tubular cells and collagen deposition in fibroblasts.

How might these results change the focus of research or clinical practice?

- These results focus attention on heme protein clearance in the pathogenesis of AKI after diabetic MI.
- IL-10 should be investigated as a therapeutic agent to prevent AKI after diabetic MI.

INTRODUCTION

Acute kidney injury (AKI) is a common complication of acute myocardial infarction (MI). Approximately 10%–20% of patients with MI develop AKI during their MI hospitalization and AKI is associated with increased mortality after MI. In fact, AKI is a major adverse prognostic factor after MI and is associated with impaired in-hospital and long-term outcomes.[1–3]

Diabetes mellitus (DM) is an important risk factor for MI and AKI after MI. Although previous studies have shown that the incidence of AKI after MI is significantly higher in patients with DM than those without DM,[4] the mechanisms underlying this observation are not well understood and therefore specific therapeutic strategies have not been elucidated. Furthermore, although iodinated contrast media have been typically implicated in AKI following MI, this association has recently been challenged and other mechanisms may underlie AKI following MI.[1 5]

In our previous study, we observed that cell-free hemoglobin (Hb) is increased in the mouse circulation after MI and increased to a greater degree in diabetic mice compared with

non-diabetic control mice.[6] Heme proteins are essential molecular regulators of oxygen transport and normally reside inside cells. After MI these heme proteins are released from dead erythrocytes and cardiomyocytes, mainly in the form of Hb and myoglobin[7] as well as other heme proteins such as cytochrome proteins, and these proteins enter into the systemic circulation.[6] Circulating cell-free heme proteins are filtered by kidney glomeruli and deposited in the proximal tubules. This exposes the kidneys to heme protein-induced injuries.[8 9] Cell-free heme proteins directly cause cell death through activation of oxidative stress and unfolded protein response in the renal cortex.[9] In addition, cell-free heme proteins function as damage-associated molecular patterns and activate renal inflammatory response and result in renal fibrosis.[10 11]

Heme proteins are scavenged in the circulation and then cleared in the form of haptoglobin–Hb complexes via the CD163 receptor in the reticuloendothelial system or heme–hemopexin complexes via the CD91 receptor on hepatocytes. Prior studies have demonstrated that diabetes impairs heme clearance mechanisms through downregulating CD163 in monocytes[12 13] and in atherosclerotic plaques.[14] However, the role of CD163 + macrophages in diabetic kidney disease and AKI is controversial.[15 16]

Interleukin 10 (IL-10) is a potent anti-inflammatory cytokine and suppresses various proinflammatory mediators.[17] Reduced circulating IL-10 levels were found in patients with type 1 and type 2 diabetes.[18 19] Recent studies have demonstrated the protective role of IL-10 in cardiac dysfunction and remodeling following acute MI through inhibition of fibrosis and enhancement of capillary density.[20 21] Our prior work demonstrated a protective effect of IL-10 in diabetic MI through upregulation of heme clearance pathways.[6] However, it remains unclear whether systemic IL-10 treatment would provide protection against kidney injury after diabetic MI.[15 16] This study was undertaken to investigate the pathogenesis of AKI after MI and to determine the therapeutic efficacy of IL-10 for renal protection after diabetic MI.

MATERIALS AND METHODS

Mice

Mice were obtained from The Jackson Laboratory (Bar Harbor, Maine, USA) and handled in accordance with the NIH Guide for the care and Use of Laboratory Animals and the ARRIVE (Animal Research: Reporting of In Vivo Experiments) guidelines.

Induction of type 1 diabetes

Adult male C57/B6 mice at the age of 8 weeks were given daily intraperitoneal injections of streptozotocin (STZ; Sigma-Aldrich, St Louis, Missouri, USA) at a dose of 50 mg/kg body weight for 5 consecutive days. STZ was dissolved in sterile citrate buffer (50 mmol/L sodium citrate, pH 4.5). Control mice were injected with pure citrate buffer for the same period. Fasting glucose levels were determined at baseline and 2 weeks after the last injection of STZ using a glucose analyzer (CareTouch Blood Glucose Monitoring System, Future Diagnostics LLC). Mice with fasting glucose level >300 mg/dL were considered diabetic and used for subsequent experiment.

Study design

There were two experimental protocols. The first protocol compared kidney injury between diabetic and control mice after MI (figure 1A protocol schematic). Diabetic mice and control mice were randomly assigned to sham surgery or MI surgery. Mice were sacrificed 3 days after the surgery. The second protocol studied the treatment effect of IL-10 on kidney injury after MI in diabetes (figure 2A schematic). Immediately after MI, diabetic mice were randomized to one of three treatment conditions: vehicle (0.1% bovine serum albumin (BSA) in phosphage buffered saline (PBS)), IL-10 (R&D Systems, Minneapolis, Minnesota, USA), or IL-10 plus Tin Protoporphyrin (SnPP, Frontier Scientific, Logan, Utah, USA). Sham controls were also conducted. Surgeons were blinded to treatment assignment and treatment assignment was randomized. IL-10 was subcutaneously injected at a dose of 50 µg/kg on days 0, 1, 3, 5, and 7 post-MI. SnPP was intraperitoneally injected at a dose of 25 mg/kg at the same time with IL-10 in mice assigned to this group.[6]

MI model

Mice were subjected to MI by ligation of left anterior descending coronary artery (LAD) as described previously.[6] Briefly, mice were anesthetized with 2%–3% isoflurane, orally intubated with a 22G IV catheter, and ventilated with a respirator (Harvard Apparatus, Cambridge, Massachusetts, USA). Buprenorphine SR (0.5 mg/kg) was injected subcutaneously before the operation to provide analgesia. A left intercostal thoracotomy was performed, and the pericardium was opened. Then, the LAD was located and ligated distal to the bifurcation between LAD and diagonal branch under a dissecting microscope. The lung was inflated before the chest was closed. The mice in sham group underwent the same operation except for the LAD ligation.

Urine iron measurement

Urine samples from mice 3 days after MI were used to determine urine iron after MI. Urine iron was measured using QuantiChrom Iron Assay Kit (DIFE-250, BioAssay Systems, Hayward, California, USA) following manufacturer's protocol. Urine iron level was normalized to urine creatinine level which was measured using QuantiChrom Creatinine Assay Kit (DICT-500, BioAssay Systems).

Kidney injury quantification and qualification

NGAL staining was used to assess AKI 3 days post-MI surgery. Integrated optical density values of NGAL-positive staining were quantified using ImageJ software (National Institutes of Health (NIH), Bethesda, Maryland, USA). Those slides were also assessed by a pathologist who was blinded to the group information using the following qualitative scoring system[22 23]: 0=no staining, 1=<25% area with positive staining, 2=25%–49% area with positive staining, 3=50%–74% area with positive staining, 4=75%–100% area with positive staining.

Infarct size calculation

Masson's trichrome stained heart sections at 3 days after MI were used to calculate infarct size. We used the circumference method as described previously.[24] Briefly, the left ventricle myocardial midline circumference was measured at the center

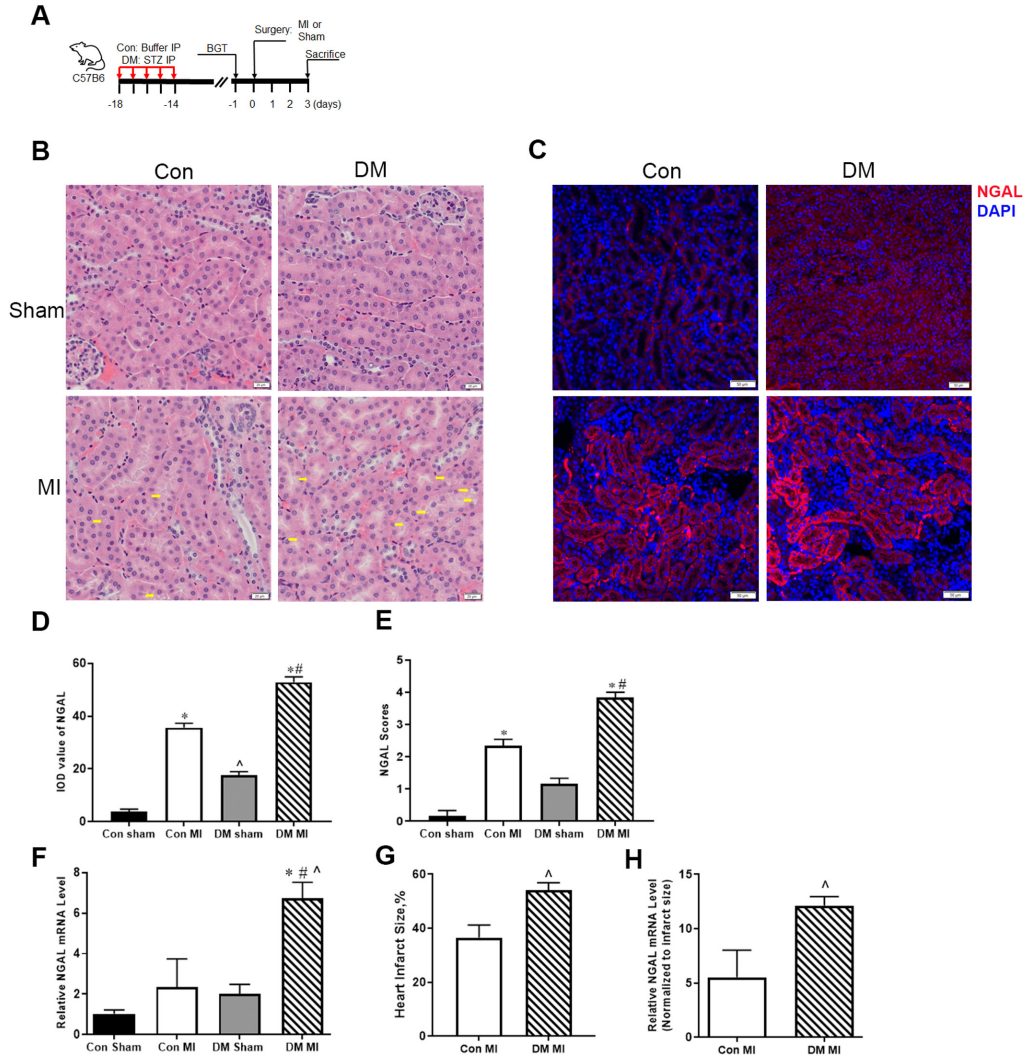

Figure 1 Diabetes is associated with worse kidney injury after acute MI. (A) Study protocol schematic. Streptozotocin (STZ) was administered via intraperitoneal (IP) injection for 5 consecutive days to induce diabetes mellitus (DM). Two weeks after the last dose of STZ or control buffer, blood glucose testing (BGT) was performed to confirm diabetes. Next, DM and control (Con) mice underwent myocardial infarction (MI) surgery or sham surgery, and organs were collected 3 days after the surgery. (B) Renal histopathology (hematoxylin and eosin staining) demonstrates vacuolization (→) in the renal cortex on day 3 post-MI. Scale bar=20 µm. (C) Immunofluorescent images of neutrophil gelatinase-associated lipocalin (NGAL, red) and 4, 6-diamidino-2-phenylindole (DAPI, blue) on day 3 post-MI. Scale bar=50 µm. (D) Quantification of NGAL-positive staining area in the renal cortex per 20× field on day 3 post-MI using image optical density (IOD). (E) Qualitative scores of NGAL expression in per 20× field on day 3 post-MI. n=6 per group. (F) mRNA expression of NGAL in kidney tissue on day 3 post-MI. (G) Infarct size calculated from heart Masson's Trichrome staining on day 3 post-MI. n=4 per group. (H) mRNA expression of NGAL in kidney tissue normalized to the myocardial infarct size for each mouse. n=4 per group. Data presented as mean±SEM and were compared by one-way analysis of variance followed by Tukey's test (D, F), the Kruskal-Wallis test followed by Dunn's post hoc test (E), and unpaired t-test (G, H). *p<0.05 vs Con sham; #p<0.05 vs DM sham; ^p<0.05 vs Con MI. BGT, blood glucose testing; Con, non-diabetic control; DM, diabetes mellitus; NGAL, neutrophil gelatinase-associated lipocalin; STZ, streptozotocin.

between the epicardial and endocardial surfaces. Infarct length was measured at the midline of infarct area. Infarct size was calculated by dividing the midline infarct length by the midline circumference and multiplying by 100. The measurements were performed with ImageJ (NIH).

Measurement of renal fibrosis

Masson's trichrome stained kidney sections at 28 days after MI were used to estimate the severity of kidney fibrosis. ImagePro Plus V.6.3 software (Media Cybernetics, Bethesda, Maryland, USA) was used for quantitative morphometric analysis of kidney fibrosis in stained sections. The average fibrosis area from five randomly selected fields per kidney was used for statistical analysis to determine significant differences.

Immunofluorescence staining and immunohistochemistry analysis

For immunofluorescence staining, trilogy solution (920P-09, Cell Marque, Rocklin, California, USA) was used on formalin-fixed paraffin-embedded kidney sections for deparaffinization, rehydration, and unblinding following

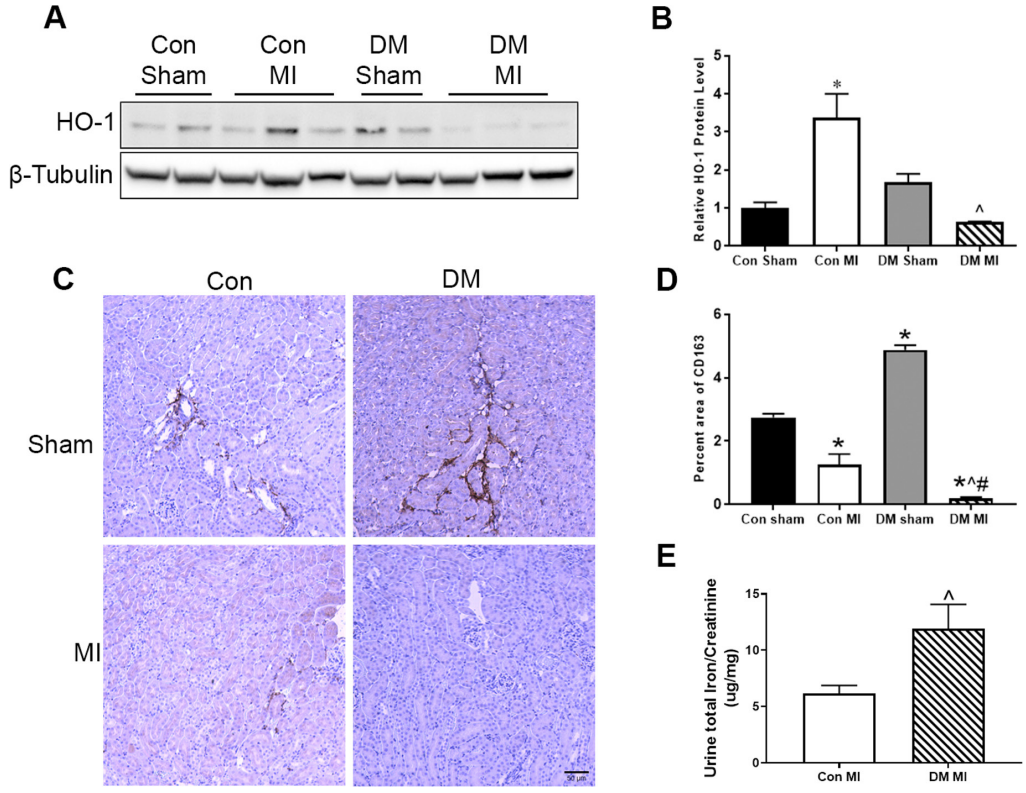

Figure 2 Inadequate renal heme clearance system after diabetic myocardial infarction (MI). Animals were treated as elaborated in figure 1. (A) Representative immunoblots of heme oxygenase 1 (HO-1) in kidney on day 3 post-MI. (B) Relative abundance of HO-1 in immunoblots expressed as fold change of densitometric ratios of HO-1/β-tubulin compared with sham-operated control mouse. (C) Immunohistochemistry image of CD163 on day 3 post-MI. Scale bar=50 µm. (D) Per cent of CD163-positive staining area per 20× field on day 3 post-MI. (E) Increased urine total iron/creatinine ratio on day 3 after MI. Data (n=6) represent mean±SEM and were compared by one-way analysis of variance followed by Tukey's test. *p<0.05 vs Con sham; #p<0.05 vs DM sham; ^p<0.05 vs Con MI. DM, diabetes mellitus.

manufacturer's instruction. The sections were then incubated overnight at 4°C with primary antibody against lipocalin-2/NGAL (ab63929, Abcam, Cambridge, UK) and Alxa543-conjugated secondary antibodies. Sections were counterstained with 4, 6-diamidino-2-phenylindole and visualized using a fluorescence microscope.

For immunohistochemistry staining, the sections were deparaffinized in xylene and rehydrated. Antigen retrieval was processed in citrate unblinding solution (14746P, Cell Signaling Technology, Danvers, Massachusetts, USA) following manufacturer's instruction. Immunohistochemical staining was performed using primary antibodies against CD163 (ab182422, Abcam) and lipocalin-2/NGAL (ab63929, Abcam), followed by incubation with respective secondary antibody and sections were examined under microscope.

Western immunoblot analysis

The kidney tissues were homogenized in Radioimmunoprecipitation Assay Lysis Buffer System (sc-24948, Santa Cruz, Dallas, Texas, USA) following manufacturer's instruction. Protein samples were processed as previously described.[6] The antibodies against CD163 (ab182422, Abcam), lipocalin-2/NGAL (ab63929, Abcam), and heme oxygenase 1 (HO-1; ADI-OSA-110-D, Enzo) were used as primary antibodies. The corresponding GAPDH (14C10, Cell Signaling Technology) or β-tubulin (ab6046, Abcam) of each sample was used as the loading control.

Quantitative RT-PCR

For gene expression level of CD163, mRNA was extracted from kidneys with RNA-STAT60 (Tel-Test, Friendswood, Texas, USA) and reverse transcribed with iScript cDNA Synthesis Kit (Bio-Rad Laboratories, Hercules, California, USA). The amplification was performed using TaqMan Gene Expression Assay (Mm00474091_m1, Applied Biosystems, Foster City, California, USA) on a TaqMan 7300 PCR machine (Applied Biosystems). For gene expression level of NGAL, mRNA was extracted from kidneys with RNeasy Mini Kit (74104, Qiagen, Hilden, Germany), reverse transcribed with RT 2 First Strand Kit (330401, Qiagen), and quantified using TaqMan Gene Expression Assay (Mm01324470_m1, Applied Biosystems) on Rotor-Gene Q 2plex Platform (Qiagen). Comparative cycle threshold method was used to calculate the relative mRNA expression of target genes. Endogenous18S rRNA (4319413E, Applied Biosystems) was used as control gene to normalize the mRNA expression of target genes.

Cell culture

Murine bone marrow cells were isolated from 8-week-old to 12-week-old C57BL/6J mice using standard

protocols.[25] Briefly, femurs and tibias were aseptically harvested from the hind limbs and bone marrow cells were flushed from each bone with DMEM containing 15% fetal bovine serum. Isolated bone marrow was gently homogenized by passing the solution through a 30 mL syringe with 18-gauge needle, and cells were cultured in DMEM containing 15% fetal bovine serum, 1% penicillin–streptomycin, and 30% L929 supernatants at 37°C with 5% CO_2. Cells were differentiated to macrophages, as previously described.[25] Bone marrow-derived macrophages (BMDM) were cultured in hyperglycemic (25 mM) DMEM with 10% fetal bovine serum and 1% penicillin–streptomycin during the treatment.

HK-2 human renal proximal tubular cells and mouse embryonic fibroblasts (MEF) were courtesy from Dr Jiang Tian (University of Toledo, Toledo, Ohio, USA). Cells were cultured in DMEM supplemented with 10% fetal bovine serum and 100 U/mL penicillin–streptomycin as complete growth media. The treatment groups for both cell culture experiments include control, 10 µM of Hb, 10 ng/mL of IL-10 (217-IL-025, R&D System), and combination of IL-10 with Hb.

Reactive oxygen species detection

HK-2 cells were cultured in a 96-well plate for 24 hours and then treated with 10 µM of Hb and/or 10 ng/mL of IL-10 for another 24 hours. The reactive oxygen species (ROS) was then measured using an ROS Detection Assay Kit (K936, BioVision, Milpitas, California) following the manufacturer's protocol.

Statistical analysis

All values are expressed as mean±SEM, and a p value <0.05 was considered statistically significant. Statistical analysis was conducted by GraphPad Prism V.8. For comparisons between two groups, an independent t-test was conducted. For comparisons among three or four groups, one-factor analysis of variance (ANOVA) was used and followed by the post hoc analysis when ANOVA overall $p<0.05$.

RESULTS

Diabetes is associated with worse renal injury after MI

To investigate renal injury after MI in diabetes, MI or sham surgery was performed in STZ-induced diabetic or control mice following the experimental protocol (figure 1A protocol schematic). We first assessed renal injury 3 days after MI on hematoxylin and eosin staining of the kidney section. Since renal injury after MI is an indirect injury, we did not detect severe renal tubular injury pathology findings such as tubular dilation or sloughing, but we observed cell vacuolization in the renal cortex, which is an early marker of AKI,[26] after MI, especially in diabetic mice (figure 1B). Consistent with the indirect injury, cystatin C was not significantly different between diabetic and control mice on day 1 or day 3 after MI (data not shown). In contrast, measurement of NGAL immunofluorescence and quantitative PCR showed significant higher NGAL expression in the kidney after MI in diabetic mice than in control mice (figure 1C–F). Specifically, the renal NGAL mRNA expression in diabetic mice increased 3.3-fold after MI surgery compared with diabetic sham control ($p<0.05$) (figure 1F). Furthermore, renal NGAL expression was 2.8-fold higher in diabetic MI compared with control MI ($p<0.05$). Diabetes may affect myocardial infarct size and subsequently affect kidney injury. Therefore, we assessed myocardial infarct size at 3 days after MI and found an increased myocardial infarct size in diabetic MI compared with control MI (figure 1G), which is in agreement with prior findings.[27 28] Next, we adjusted for the potential confounding effect of myocardial infarct size on kidney injury by normalizing NGAL expression to infarct size. Diabetic MI still had significantly higher renal NGAL expression compared with control MI, even after normalization to infarct size (figure 1H). Overall, these findings demonstrate worse renal injury in diabetic MI compared with control MI.

Impaired heme protein scavenging system in diabetic mice after MI

Given prior evidence of increased circulating cell-free Hb after MI in diabetic mice,[6] we examined the heme protein scavenging system in the kidneys of diabetic and control mice at baseline and after MI. We measured scavenger receptor CD163 and HO-1 expression, the rate-limiting enzyme in heme scavenging and degradation pathway. Baseline renal HO-1 and CD163 expression are higher in diabetic mouse than in control mouse (figure 2A–D). MI significantly increased renal HO-1 expression in control mice. However, in diabetic MI, HO-1 was not significantly upregulated (figure 2A,B). Interestingly, renal CD163 was upregulated in diabetic sham, but significantly decreased after diabetic MI (figure 2C,D). These results demonstrate that diabetes affects renal heme clearance at baseline and after diabetic MI. Importantly, the critical components of the renal heme processing system, namely HO-1 and CD163, were impaired after diabetic MI. We further measured the urine iron level to determine renal iron burden after MI in control and diabetic mice. We found that the urine iron level was significantly higher in diabetic MI than in control MI (figure 2E), indicating a higher load of iron stress after diabetic MI and inadequate heme clearance in diabetic MI.

IL-10 attenuates renal inflammation and improves renal heme scavenging after diabetic MI

To test the treatment effect of IL-10 on kidney injury after diabetic MI, diabetic mice underwent MI surgery and were treated with vehicle, IL-10, or combination of IL-10 and tin protoporphyrin (SnPP), an HO-1 activity inhibitor following the protocol described in figure 3A.

IL-10 significantly improved heart function 28 days after treatment but had limited effect on ejection fraction 7 days after treatment (figure 3B). In contrast, MI dramatically induced early renal expression of proinflammatory cytokines and chemokines, including interleukin-1 beta (IL-1B) and monocyte chemoattractant protein-1 (MCP-1) ($p<0.05$) in diabetic mice on day 3 after MI (figure 3C,D). IL-10 significantly reduced MCP-1 expression, and this effect was partially blocked by SnPP. Therefore, the early reductions in renal inflammatory and chemokine response to MI noted with IL-10 treatment are independent of IL-10

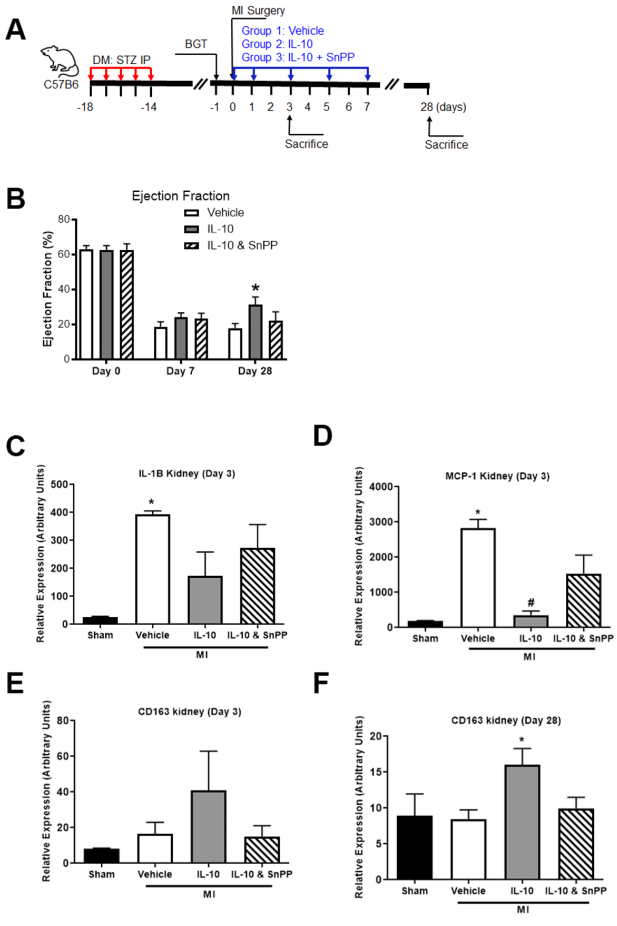

Figure 3 IL-10 inhibits renal inflammatory gene expression and promotes renal CD163 expression after diabetic myocardial infarction (MI). (A) Study protocol schematic. STZ-induced diabetic mice underwent MI surgery and were randomly assigned to one of three MI treatment groups: vehicle control, IL-10, or combination of IL-10 and SnPP. Each treatment was administered at days 0, 1, 3, 5, and 7 after MI. Mice were sacrificed 3 days after MI for short-term assessments or on day 28 after MI for long-term assessments. Heart function was assessed on days 0, 7, and 28 days after MI with echocardiography. (B) IL-10 treatment had no significant effect on heart ejection fraction (EF) at the early time point (day 7) after MI, but significantly improved EF at the late timepoint (day 28) after MI. (C–E) Gene expression of IL-1B, MCP-1, and CD163 in kidney on day 3 after diabetic MI. (F) Gene expression of CD163 in kidney on day 28 after diabetic MI. Data (n=6 per group) represent mean±SEM and were compared by one-way analysis of variance followed by Tukey's test. *p<0.05 vs sham, #p<0.05 vs MI+vehicle. BGT, blood glucose testing; DM, diabetes mellitus; IL-10, interleukin 10; MCP-1, monocyte chemoattractant protein-1; STZ, streptozotocin.

effects on cardiac function, which were observed at the later 28-day timepoint. We can conclude that IL-10 has a direct effect on early post-MI renal inflammatory signaling independent of its effect on cardiac function. We further measured the expression of renal CD163 in diabetic MI. IL-10 treatment showed a trend to increased CD163 mRNA expression in diabetic kidneys on day 3 post-MI (figure 3E), and this effect was statistically significant on day 28 post-MI ($p<0.05$ vs sham, figure 3F).

IL-10 reduces renal fibrosis and albuminuria after diabetic MI

Renal fibrosis were quantified using Masson's Trichrome staining 28 days after MI in IL-10-treated diabetic mice to assess the long-term effect of IL-10. As depicted in figure 4A–C, IL-10 significantly reduced renal fibrosis ($p<0.05$, vs vehicle) in diabetic mice at day 28 post-MI, and this protective effect of IL-10 was partially blocked by SnPP.

The urine albumin to creatinine (UAC) ratio was used to further assess chronic renal injury. As shown in figure 4D, UAC ratio was significantly increased post-MI (vehicle vs sham, $p<0.05$), and the UAC ratio in IL-10 treatment group was dramatically reduced compared with vehicle group ($p<0.05$). This protective effect of IL-10 was blocked by SnPP ($p<0.05$ vs vehicle). In summary, IL-10 provides robust protection against MI-related renal fibrosis and albuminuria in diabetic mice.

IL-10 reduces Hb-induced ROS and upregulates Hb-induced HO-1

To study the mechanism of the protective effect of IL-10 against renal injury after diabetic MI, we investigated the effect of IL-10 on cell-free Hb-induced cellular injury and heme clearance pathways using in vitro models. First, ROS was measured in renal proximal tubular cells (HK-2 cells) treated with Hb and IL-10. Hb significantly induced ROS in HK-2 cells. Furthermore, IL-10 treatment partially reversed the ROS induced by Hb (figure 5A). HO-1 was also measured to study the heme clearance pathways in HK-2 cells. As shown in figure 5B,C, HO-1 was significantly induced by Hb, and this effect was potentiated by IL-10 treatment, indicating that IL-10 improves heme clearance in proximal tubular cells.

The effect of IL-10 on heme clearance pathways was further investigated in BMDM. Cultured BMDM were treated with Hb and IL-10 under high glucose condition. As depicted in figure 5D,E, Hb significantly increased HO-1 protein expression in BMDM under high glucose condition (25 mM). Moreover, induction of HO-1 was potentiated when BMDM were co-treated with IL-10 and Hb under high glucose condition. This finding was further validated by quantitative PCR analysis of HO-1 mRNA expression in BMDM (figure 5F). These data demonstrate induction of HO-1 expression under diabetic conditions after treatment with IL-10 and potentiation of the Hb-induced expression of HO-1 by IL-10.

IL-10 inhibits Hb-induced collagen synthesis

Reactive iron has been reported to induce collagen synthesis in hepatic fibroblasts.[29] Therefore, we investigated the role of Hb and IL-10 in fibrogenesis in vitro. We assessed the effect of Hb on collagen synthesis in a mouse fibroblast cell line, MEF. As shown in figure 6A,B, Hb significantly induced collagen synthesis, and such collagen production was blocked by co-treatment of Hb and IL-10. Therefore, IL-10 provides protection against heme-induced fibrosis.

DISCUSSION

In this study, we demonstrated greater renal injury after MI in diabetic mice compared with control mice after MI.

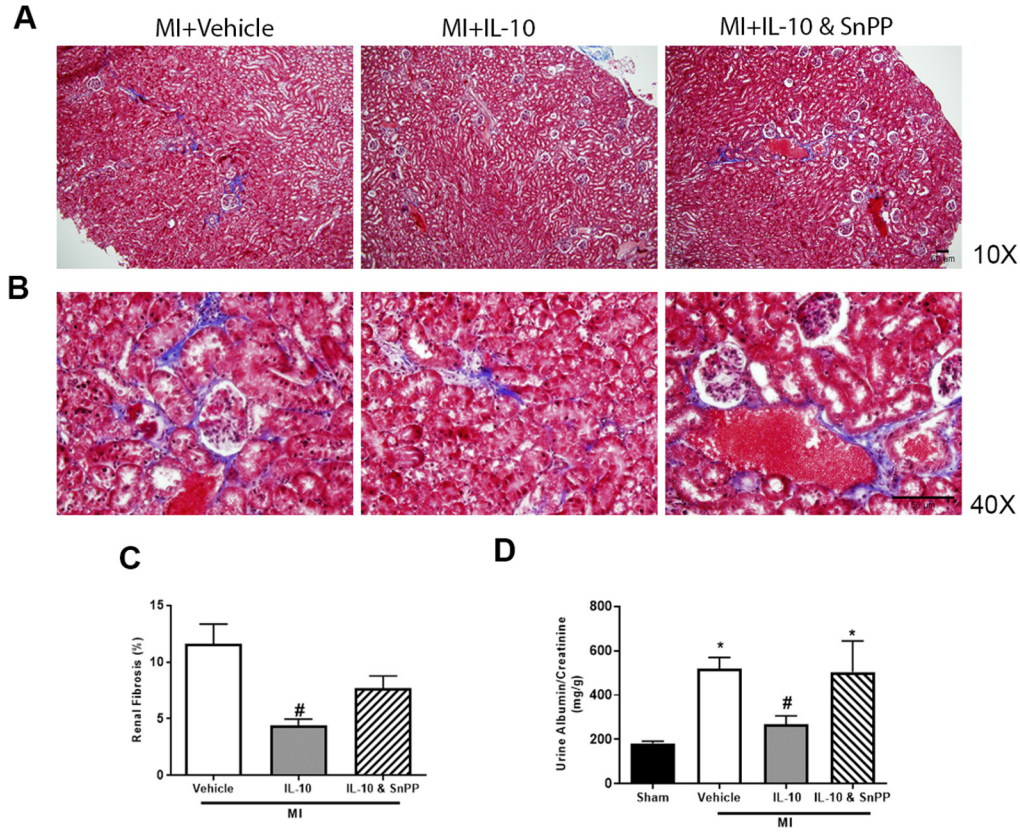

Figure 4 IL-10 reduces renal fibrosis and urine albumin after diabetic myocardial infarction (MI). Animals were treated as described in figure 3. (A) Representative Masson's Trichrome staining images in renal cortex on day 28 post-MI. Scale bar=50 µm. (B) Larger magnification (40×) of representative images. Scale bar=50 µm. (C) Quantification of renal fibrosis area in Masson's Trichrome staining images per 20× field on day 28 post diabetic MI. (D) Urine albumin/creatinine ratio on day 28 after diabetic MI. Data (n=6 per group) represent mean±SEM and were compared by one-way analysis of variance followed by Tukey's test. *p<0.05 vs sham; #p<0.05 vs MI+vehicle. IL-10, interleukin 10.

Furthermore, we found impaired renal heme clearance pathways after diabetic MI. These findings demonstrate that diabetes is a vulnerable condition for AKI after MI, and this observation may be mediated by increased circulating cell-free Hb and inadequate renal heme clearance pathways. In addition, we demonstrated that systemic IL-10 treatment can reduce acute kidney inflammation and chronic renal fibrosis and albuminuria after diabetic MI. IL-10 also upregulates HO-1 expression in macrophages and renal proximal tubular cells in the presence of Hb. Notably, we reported that Hb, which is known to increase in the circulation after MI,[6] can directly induce collagen deposition in mouse fibroblasts and IL-10 inhibits this collagen production.

AKI is a common complication after MI, with a prevalence of 10%–20%,[30–33] and is strongly associated with morbidity and mortality.[2 34 35] However, the mechanisms causing AKI after MI are multifactorial in nature and have not been fully understood. Clinical studies have indicated that renal hypoperfusion, usage of nephrotoxic agents such as iodinated contrast, hypertension, DM, infection, and the performance of coronary artery bypass graft surgery are important risk factors for AKI after MI.[36 37] Although iodinated contrast has typically been implicated in AKI after MI treated with percutaneous coronary intervention, recent studies have questioned this association and other factors may be responsible for AKI after MI.[1 5] Our findings implicate inadequate heme protein clearance as a novel pathogenic mechanism for AKI after diabetic MI.

Clinical studies utilizing cardiac MRI have demonstrated significant myocardial hemorrhage after MI, a previously underappreciated phenomenon.[38–41] Intramyocardial hemorrhage was associated with larger infarct size, worse left ventricular systolic function, and higher rates of death.[42] Furthermore, heme proteins also enter the circulation after MI, as demonstrated in our prior work.[6] Circulating heme proteins are extensively and rapidly filtered and deposited in kidneys and result in acute and chronic kidney injury.[43–45] Circulating heme proteins are toxic and are mainly sequestered and degraded to metabolites by the heme protein scavenger system.[46] The scavenger system is a multiple component pathway made up of several soluble plasma proteins (eg, haptoglobin, hemopexin, α1-microglobulin, and albumin),[47] cell-based receptors (eg, CD163 and CD91), the monocyte/macrophage cell system,[48 49 50] and intracellular heme oxygenases (eg, HO-1 and HO-2).

In patients with diabetes, CD163 expression in monocytes is significantly lower than in patients without diabetes.[12 13] However, such impairment of heme scavenger system in kidney disease is controversial.[15 16] In the current study, we found that renal CD163 and HO-1 expression were higher

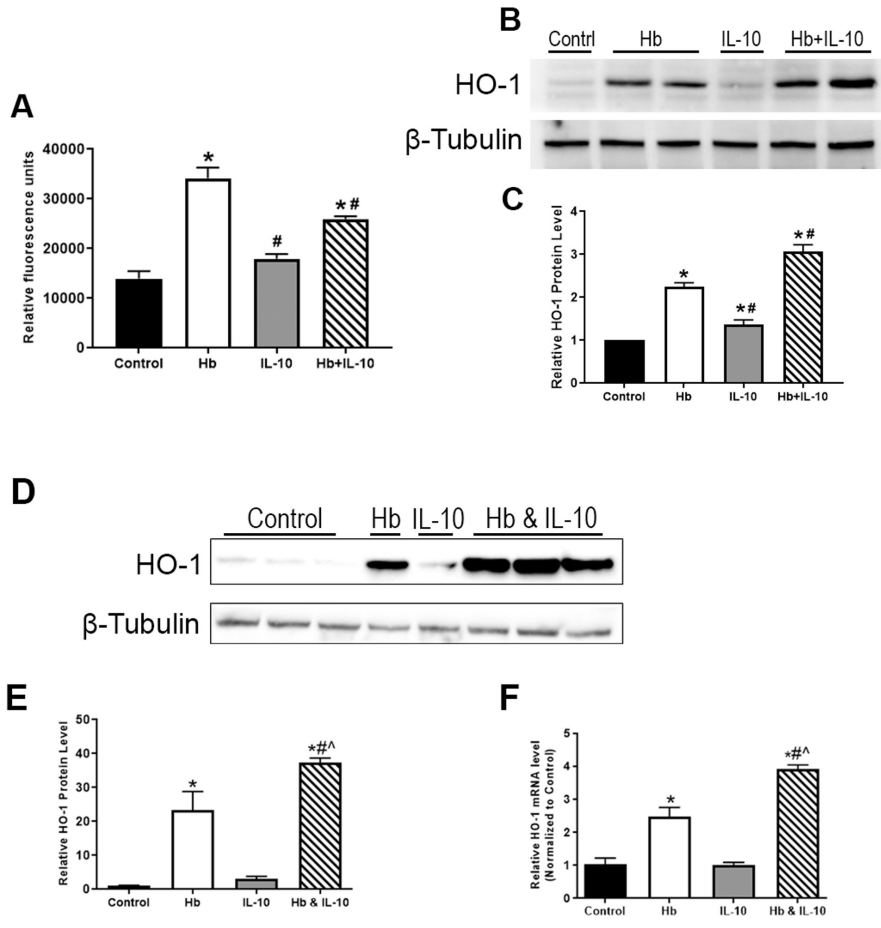

Figure 5 IL-10 reduces ROS and upregulates HO-1 after hemoglobin (Hb) treatment. Renal proximal tubular cells (HK-2) were treated with Hb (10 µM), IL-10 (10 ng/mL), or combination of Hb and IL-10. (A) Cellular ROS were measured at 24 hours after treatment. (B) Cell homogenates were processed for immunoblot analysis for the expression of HO-1 expression in HK-2 cells 24 hours after treatment. (C) Relative abundance of HO-1 in immunoblots expressed as fold change of densitometric ratios of HO-1/β-tubulin compared with control cells. (D) Mouse bone marrow-derived macrophages (BMDM) were treated with Hb (10 µM), IL-10 (10 ng/mL), or combination of Hb and IL-10 for 24 hours. Representative immunoblots of HO-1 protein expression in BMDM after treatment were shown. (E) Relative abundance of HO-1 in immunoblots expressed as fold change of densitometric ratios of HO-1/β-tubulin compared with control cells. (F) mRNA expression of HO-1 in BMDM after treatment. Data (n=5 per group) represent mean±SEM and were compared by one-way analysis of variance followed by Tukey's test. *p<0.05 vs control, #p<0.05 vs Hb, ^p<0.05 vs IL-10. HO-1, heme oxygenase 1; IL-10, interleukin 10; ROS, reactive oxygen species.

in diabetic mice than in control mice at baseline (figure 2). However, after MI, there was almost complete absence of CD163 staining in diabetic kidneys. Similarly, MI significantly induced renal HO-1 expression in control mice, but not in diabetic mice. These novel results suggest that diabetes may create a unique susceptibility to AKI due to vulnerability to heme toxicity. In support of the critical role of heme protein processing, Abo *et al*[51] observed protection against diabetic renal disease via induction of renal HO-1 expression. HO-1 is the final step in the scavenging and clearance of toxic-free heme proteins and its cardiorenal protective effects have been documented in prior studies.[51 52] Overall, our findings implicate inadequate heme clearance pathways in the pathogenesis of MI-induced AKI, a novel explanation for this common and significant disease state.

IL-10 has significant effects on two key steps in the heme processing system. First, it upregulates CD163 on macrophages and facilitates absorption of heme proteins by macrophages.[53 54] Second, it also upregulates HO-1 expression, the main intracellular enzyme responsible for degradation of heme proteins.[55] In the current study, we demonstrated that IL-10 can upregulate the expression of HO-1 and CD163 expression both in vitro and in vivo. In addition, IL-10 treatment showed the ability to potentiate the renal heme scavenging system, decrease acute renal inflammation, and prevent chronic renal fibrosis and proteinuria after diabetic MI. Importantly, MI induced significant albuminuria in diabetic mice, however IL-10 was able to almost fully prevent this effect (figure 4D).

Renal fibrosis is the common final pathway of nearly all chronic and progressive nephropathies and the best histologic predictor of renal functional decline in chronic kidney disease.[56] Inflammation is a critical trigger for renal fibrosis.[56] In this study, we demonstrated a strong antifibrotic effect of IL-10 treatment in diabetic MI (figure 4A–C). Furthermore, we also reported that Hb can induce collagen production in

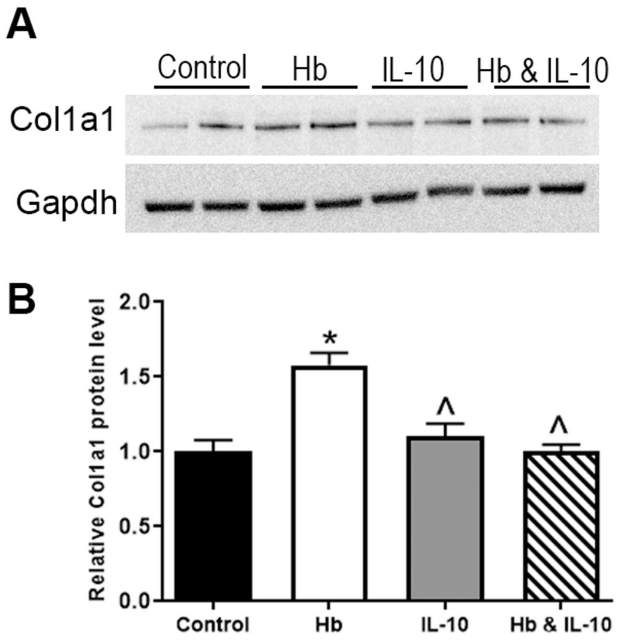

Figure 6 IL-10 attenuates hemoglobin (Hb)-induced collagen synthesis in mouse embryonic fibroblast (MEF) cells. MEF were treated with Hb (10 µM), IL-10 (10 ng/mL), or combination of Hb and IL-10 for 24 hours. (A) Representative immunoblots of collagen 1A1 (Col1A1) in MEF cells after treatment. (B) Relative abundance of Col1A1 in immunoblots expressed as fold change of densitometric ratios of Col1A1/β-tubulin compared with control cells. Data (n=4) represent mean±SEM and were compared by one-way analysis of variance followed by Tukey's test. *p<0.05 vs control; ^p<0.05 vs Hb. IL-10, interleukin 10.

mouse fibroblast cells, and such collagen production can be inhibited by IL-10. In a study conducted by Mehta *et al*,[29] iron treatment significantly increased expression of α-SMA, TGF-β, TGF-β receptor II, and phospho-Smad2, resulting in collagen deposition in hepatic stellate cells. This fibroblast activation and collagen secretion were blocked by iron chelation. Those results together with our findings highlight the direct fibrosis-inducing effects of heme proteins and iron.

Although these data provide strong support for short-term and long-term renal protective effects of IL-10 after MI in diabetes, there are some limitations to our study. Although the STZ diabetic mouse model is well-established, it has been criticized. This model was selected since we have established the murine MI model in our laboratory and have acceptable perioperative mortality rates with STZ diabetic mice in this model. The use of SnPP, a chemical HO-1 inhibitor, has well-known limitations and concerns about its specificity. MEF cell line is a general, but not a renal-specific fibroblast cell line. Overall, despite these limitations, our findings support further exploration of IL-10 as a treatment during the acute phase of diabetic MI and highlight novel mechanisms underlying the pathogenesis of renal injury after MI.

Taken together, our findings demonstrate that IL-10 provides renal protection in diabetic MI largely through upregulation of the heme clearance system. These findings underscore the importance of free heme in mediating AKI after diabetic MI and the ability of IL-10 to rescue the dysfunctional heme processing system in diabetes.

Contributors Performing the experiments: XF, XZ, LCL, AYK, SPC, XC, RG; conception and design or analysis and interpretation of data, or both: XF, XZ, LCL, XC, LDD, CJC, RG; drafting the manuscript or revising it critically for important intellectual content: XF, XZ, LCL, LDD, CJC, RG; final approval of the manuscript: XF, XZ, LCL, AYK, SPC, XC, LDD, CJC, RG; Guarantor: RG.

Funding This study was supported in part by grants from the NIH including F32 HL099283 (RG) and the American Heart Association, 09POST2230297 (RG).

Competing interests None declared.

Patient consent for publication Not applicable.

Ethics approval All experiments conformed to the protocols approved by the Institutional Animal Care and Use Committee at Northwestern University and the University of Toledo (Protocol # 108703).

Provenance and peer review Not commissioned; internally peer reviewed.

Data availability statement Data are available upon reasonable request.

ORCID iD
Rajesh Gupta http://orcid.org/0000-0001-7428-7671

REFERENCES

1 Schmucker J, Fach A, Becker M, *et al*. Predictors of acute kidney injury in patients admitted with ST-elevation myocardial infarction - results from the Bremen STEMI-Registry. *Eur Heart J Acute Cardiovasc Care* 2018;7:710–22.
2 Fox CS, Muntner P, Chen AY, *et al*. Short-term outcomes of acute myocardial infarction in patients with acute kidney injury: a report from the National cardiovascular data registry. *Circulation* 2012;125:497–504.
3 Ronco C, Cicoira M, McCullough PA. Cardiorenal syndrome type 1. *J Am Coll Cardiol* 2012;60:1031–42.
4 Marenzi G, Cosentino N, Milazzo V, *et al*. Acute kidney injury in diabetic patients with acute myocardial infarction: role of acute and chronic glycemia. *J Am Heart Assoc* 2018;7:e008122.
5 Caspi O, Habib M, Cohen Y, *et al*. Acute kidney injury after primary angioplasty: is contrast-induced nephropathy the culprit? *J Am Heart Assoc* 2017;6. doi:10.1161/JAHA.117.005715. [Epub ahead of print: 24 Jun 2017].
6 Gupta R, Liu L, Zhang X, *et al*. Il-10 provides cardioprotection in diabetic myocardial infarction via upregulation of heme clearance pathways. *JCI Insight* 2020;5. doi:10.1172/jci.insight.133050. [Epub ahead of print: 03 Sep 2020].
7 Sawicki KT, Chang H-C, Ardehali H. Role of heme in cardiovascular physiology and disease. *J Am Heart Assoc* 2015;4:e001138.
8 Nath KA, Grande JP, Farrugia G, *et al*. Age sensitizes the kidney to heme protein-induced acute kidney injury. *Am J Physiol Renal Physiol* 2013;304:F317–25.
9 Deuel JW, Schaer CA, Boretti FS, *et al*. Hemoglobinuria-related acute kidney injury is driven by intrarenal oxidative reactions triggering a heme toxicity response. *Cell Death Dis* 2016;7:e2064.
10 Van Avondt K, Nur E, Zeerleder S. Mechanisms of haemolysis-induced kidney injury. *Nat Rev Nephrol* 2019;15:671–92.
11 Giuliani KTK, Kassianos AJ, Healy H, *et al*. Pigment nephropathy: novel insights into inflammasome-mediated pathogenesis. *Int J Mol Sci* 2019;20:1997.
12 Min D, Brooks B, Wong J. *Monocyte CD163 is altered in association with diabetic complications: possible protective role*, 2016.
13 Kawarabayashi R, Motoyama K, Nakamura M, *et al*. The association between monocyte surface CD163 and insulin resistance in patients with type 2 diabetes. *J Diabetes Res* 2017;2017:6549242
14 Levy AP, Purushothaman KR, Levy NS, *et al*. Downregulation of the hemoglobin scavenger receptor in individuals with diabetes and the HP 2-2 genotype. *Circ Res* 2007;101:106–10.
15 Klessens CQF, Zandbergen M, Wolterbeek R, *et al*. Macrophages in diabetic nephropathy in patients with type 2 diabetes. *Nephrology Dialysis Transplantation* 2016;24:1322–9.
16 O'Reilly VP, Wong L, Kennedy C, *et al*. Urinary soluble CD163 in active renal vasculitis. *J Am Soc Nephrol* 2016;27:2906–16.
17 Hedrich CM, Bream JH. Cell type-specific regulation of IL-10 expression in inflammation and disease. *Immunol Res* 2010;47:185–206.
18 Yaghini N, Mahmoodi M, Asadikaram GR, *et al*. Serum levels of interleukin 10 (IL-10) in patients with type 2 diabetes. *Iran Red Crescent Med J* 2011;13:752.

19 Myśliwska J, Zorena K, Semetkowska-Jurkiewicz E, *et al*. High levels of circulating interleukin-10 in diabetic nephropathy patients. *Eur Cytokine Netw* 2005;16:117–22.
20 Krishnamurthy P, Rajasingh J, Lambers E, *et al*. Il-10 inhibits inflammation and attenuates left ventricular remodeling after myocardial infarction via activation of STAT3 and suppression of HuR. *Circ Res* 2009;104:e9–18.
21 Interleukin 10 administration after MI improves left ventricular function in rodents. *Nat Clin Pract Cardiovasc Med* 2008;5:750.
22 Jiang C, Zhu W, Yan X, *et al*. Rescue therapy with tanshinone IIA hinders transition of acute kidney injury to chronic kidney disease via targeting GSK3β. *Sci Rep* 2016;6:36698.
23 Si J, Ge Y, Zhuang S, *et al*. Adrenocorticotropic hormone ameliorates acute kidney injury by steroidogenic-dependent and -independent mechanisms. *Kidney Int* 2013;83:635–46.
24 Takagawa J, Zhang Y, Wong ML, *et al*. Myocardial infarct size measurement in the mouse chronic infarction model: comparison of area- and length-based approaches. *J Appl Physiol* 2007;102:2104–11.
25 Wu X, Ren G, Gunning WT, *et al*. FmvB: a Francisella tularensis Magnesium-Responsive outer membrane protein that plays a role in virulence. *PLoS One* 2016;11:e0160977.
26 Si J, Ge Y, Zhuang S, *et al*. Adrenocorticotropic hormone ameliorates acute kidney injury by steroidogenic-dependent and -independent mechanisms. *Kidney Int* 2013;83:635–46.
27 Issan Y, Kornowski R, Aravot D, *et al*. Heme oxygenase-1 induction improves cardiac function following myocardial ischemia by reducing oxidative stress. *PLoS One* 2014;9:e92246.
28 Di Filippo C, Marfella R, Cuzzocrea S, *et al*. Hyperglycemia in streptozotocin-induced diabetic rat increases infarct size associated with low levels of myocardial HO-1 during ischemia/reperfusion. *Diabetes* 2005;54:803–10.
29 Mehta KJ, Coombes JD, Briones-Orta M, *et al*. Iron enhances hepatic fibrogenesis and activates transforming growth factor-β signaling in murine hepatic stellate cells. *Am J Med Sci* 2018;355:183–90.
30 Hwang SH, Jeong MH, Ahmed K, *et al*. Different clinical outcomes of acute kidney injury according to acute kidney injury network criteria in patients between ST elevation and non-ST elevation myocardial infarction. *Int J Cardiol* 2011;150:99–101.
31 Marenzi G, Assanelli E, Campodonico J, *et al*. Acute kidney injury in ST-segment elevation acute myocardial infarction complicated by cardiogenic shock at admission. *Crit Care Med* 2010;38:438–44.
32 Tsai TT, Patel UD, Chang TI, *et al*. Contemporary incidence, predictors, and outcomes of acute kidney injury in patients undergoing percutaneous coronary interventions: insights from the NCDR Cath-PCI registry. *JACC Cardiovasc Interv* 2014;7:1–9.
33 Shacham Y, Leshem-Rubinow E, Steinvil A, *et al*. Renal impairment according to acute kidney injury network criteria among ST elevation myocardial infarction patients undergoing primary percutaneous intervention: a retrospective observational study. *Clin Res Cardiol* 2014;103:525–32.
34 Benjamin EJ, Muntner P, Alonso A, *et al*. Heart disease and stroke Statistics-2019 update: a report from the American heart association. *Circulation* 2019;139:e56–28.
35 Chertow GM, Burdick E, Honour M, *et al*. Acute kidney injury, mortality, length of stay, and costs in hospitalized patients. *J Am Soc Nephrol* 2005;16:3365–70.
36 Koreny M, Karth GD, Geppert A, *et al*. Prognosis of patients who develop acute renal failure during the first 24 hours of cardiogenic shock after myocardial infarction. *Am J Med* 2002;112:115–9.
37 Levin A, Warnock DG, Mehta RL, *et al*. Improving outcomes from acute kidney injury: report of an initiative. *Am J Kidney Dis* 2007;50:1–4.
38 Aguor ENE, Arslan F, van de Kolk CWA, *et al*. Quantitative T 2* assessment of acute and chronic myocardial ischemia/reperfusion injury in mice. *MAGMA* 2012;25:369–79.
39 Chen W, Zhang B, Xia R, *et al*. T2 mapping at 7T MRI can quantitatively assess intramyocardial hemorrhage in rats with acute reperfused myocardial infarction in vivo. *J Magn Reson Imaging* 2016;44:194–203.
40 Eitel I, Kubusch K, Strohm O, *et al*. Prognostic value and determinants of a hypointense infarct core in T2-weighted cardiac magnetic resonance in acute reperfused ST-elevation-myocardial infarction. *Circ Cardiovasc Imaging* 2011;4:354–62.
41 Carrick D, Haig C, Ahmed N, *et al*. Myocardial hemorrhage after acute reperfused ST-segment-elevation myocardial infarction: relation to microvascular obstruction and prognostic significance. *Circ Cardiovasc Imaging* 2016;9:e004148.
42 Carberry J, Carrick D, Haig C, *et al*. Persistent Iron Within the Infarct Core After ST-Segment Elevation Myocardial Infarction: Implications for Left Ventricular Remodeling and Health Outcomes. *JACC Cardiovasc Imaging* 2018;11:1248–56.
43 Boutaud O, Moore KP, Reeder BJ, *et al*. Acetaminophen inhibits hemoprotein-catalyzed lipid peroxidation and attenuates rhabdomyolysis-induced renal failure. *Proc Natl Acad Sci U S A* 2010;107:2699–704.
44 Moore KP, Holt SG, Patel RP, *et al*. A causative role for redox cycling of myoglobin and its inhibition by alkalinization in the pathogenesis and treatment of rhabdomyolysis-induced renal failure. *J Biol Chem* 1998;273:31731–7.
45 Zager RA, Gamelin LM. Pathogenetic mechanisms in experimental Hemoglobinuric acute renal failure. *Am J Physiol* 1989;256:F446–55.
46 Schaer DJ, Buehler PW. Cell-Free hemoglobin and its scavenger proteins: new disease models leading the way to targeted therapies. *Cold Spring Harb Perspect Med* 2013;3:a013433.
47 Schaer DJ, Alayash AI. Clearance and control mechanisms of hemoglobin from cradle to Grave. *Antioxid Redox Signal* 2010;12:181–4.
48 Soares MP, Hamza I. Macrophages and iron metabolism. *Immunity* 2016;44:492–504.
49 Kristiansen M, Graversen JH, Jacobsen C, *et al*. Identification of the haemoglobin scavenger receptor. *Nature* 2001;409:198–201.
50 Schaer DJ, Schaer CA, Buehler PW, *et al*. Cd163 is the macrophage scavenger receptor for native and chemically modified hemoglobins in the absence of haptoglobin. *Blood* 2006;107:373–80.
51 Abo El Gheit R, Emam MN. Targeting heme oxygenase-1 in early diabetic nephropathy in streptozotocin-induced diabetic rats. *Physiol Int* 2016;103:413–27.
52 Otterbein LE, Foresti R, Motterlini R. Heme oxygenase-1 and carbon monoxide in the heart: the balancing act between danger signaling and pro-survival. *Circ Res* 2016;118:1940–59.
53 Sulahian TH, Högger P, Wahner AE, *et al*. Human monocytes express CD163, which is upregulated by IL-10 and identical to p155. *Cytokine* 2000;12:1312–21.
54 Williams L, Jarai G, Smith A, *et al*. Il-10 expression profiling in human monocytes. *J Leukoc Biol* 2002;72:800–9.
55 Lee T-S, Chau L-Y. Heme oxygenase-1 mediates the anti-inflammatory effect of interleukin-10 in mice. *Nat Med* 2002;8:240–6.
56 Humphreys BD. Mechanisms of renal fibrosis. *Annu Rev Physiol* 2018;80:309–26.